03

# Secondary vortices formation during the tip vortex interaction with the surface

© T.V. Konstantinovskaya, A.E. Lutsky

Keldysh Institute of Applied Mathematics, Russian Academy of Sciences, Moscow, Russia
E-mail: konstantinovskaya.t.v@gmail.com

*Received August 18, 2025*
*Revised September 18, 2025*
*Accepted September 18, 2025*

The paper considers the transformation of tip vortex and formation of secondary vortices during its interaction with the lifting surface in a supersonic flow ($M_\infty = 3$). The mechanism for the secondary vortex formation as a result of the boundary layer separation on the lifting surface has been investigated. The profiled and flat wings were considered, as well as two options of relative arrangement of the tip vortex and lifting surface. Numerical data were obtained on the multiprocessor hybrid supercomputer system K-60 in the Supercomputer Centre of Collective Usage of KIAM RAS.

**Keywords:** secondary vortices, supersonic flow, tip vortex.

DOI: 10.61011/TPL.2026.01.62831.20475

Concentrated vortices are naturally formed during flow around aircraft; their emergence is typically releated with separation regions. Concentrated (coherent) vortices are sharply localized regions in the flow where the magnitude of vorticity (velocity curl) significantly exceeds the surrounding „background“ values. The presence of such vortex structures gives rise to a number of problems that must be taken into account in designing and operating aircraft. For instance, dangers associated with tip vortices are well known in civil aviation. An aircraft caught in a wake vortex behind the aircraft moving ahead is subject to intense aerodynamic forces and moments that may lead to spontaneous variations in the heading, altitude, speed, etc., up to complete loss of control. These issues are being actively investigated both in our country and abroad [1–3]. Of no less importance is accounting for the vortex structures effect on the flow around aircraft [4]. Vortices generated in flow around the canard or wing strake may affect the flow around downstream structural elements. In a simplified model, this question was investigated in a number of works, e.g. [5–7]. Those publications, as well as a number of others, were devoted to subsonic (almost incompressible) modes. Supersonic flows of this type were considered in significantly fewer studies, and many issues require further investigation. In our earlier study ([8]), we investigated a supersonic flow (free-stream Mach number $M_\infty = 3$) around a tandem of rectangular profiled wings. Among other results, there was revealed emergence of several separations on the main wing surface accompanied by formation of secondary vortices. Arrangement of the separation regions and secondary vortices depended on an uneven pressure distribution (the presence or absence of unfavorable gradient areas) on the wing surface, which hindered identification of the main mechanism for secondary vortex formation. Therefore, this paper pays special attention to the simplest case, namely, flat wing. The main goal of this study was to solve two fundamental issues.

1. What are the sources and locations of the boundary layer separation on the wing surface, which induces secondary vortices?

2. What are the processes to which secondary vortices are subject in moving downstream, and what are the factors affecting them?

Note that the field of vortex aerodynamics is not limited to the mentioned tasks. For instance, capabilities of local control of the flow by using vortex generators of various types are currently examined [9].

This paper reports on investigation of interaction between the tip vortex and vortex sheet formed during flow around the generator wing with the rectangular main wing in a free stream with $M_\infty = 3$ and Reynolds number $Re = 1 \cdot 10^7$ (corresponding to the characteristic length of 1 m). The generator has a hexagonal profile with relative thickness of 13.3 %; its half-span is $l_1 = 0.0475$ m, chord is $b_1 = 0.03$ m, and angle of attack is $\alpha_1 = 10^\circ$. The main wing is flat; it has half-span $l_1 = 0.097$ m and two chord options $b_1 = 0.03$ m and $b_2 = 0.06$ m with the zero angle of attack. Two options for the wing and generator relative arrangement have been considered. Option 1: the generator's tip vortex intersects the main wing almost symmetrically about vertical (the main wing leading edge is 0.0018 m higher than the generator trailing edge). Option 2: the main part of the tip vortex is located beneath the wing (the main wing leading edge is 0.0026 m higher than the generator trailing edge). In the given Cartesian frame of reference, direction $Ox$ coincides with that of free stream, while the coordinate origin is located at the intersection between the main wing and plane of symmetry so that the main-wing axis coordinate is $x = 0.015$ m. Fig. 1 shows a schematic

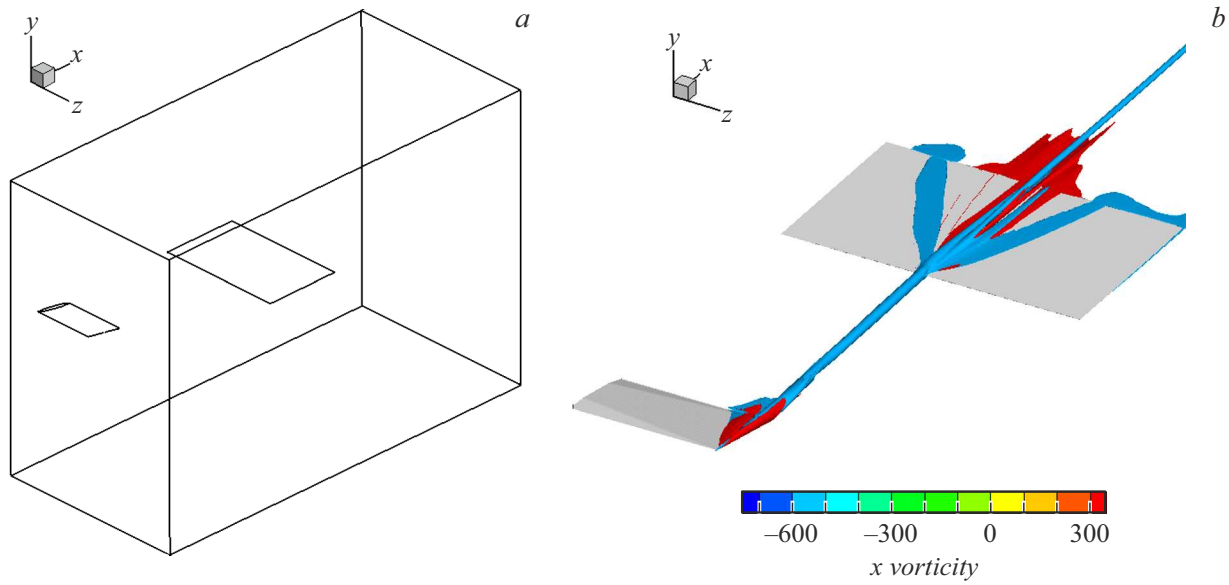


**Figure 1.** *a* — schematic representation of the computational domain, *b* — basic components of a vortex system.

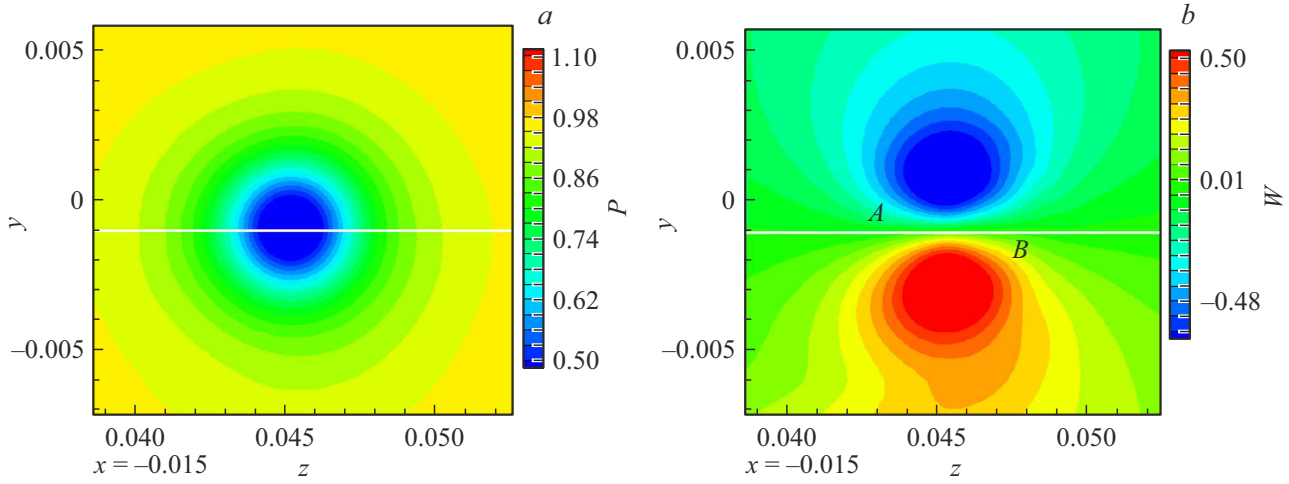


**Figure 2.** Distribution of pressure $P$ in cross-section $x = -0.015$ m ahead of the main wing edge ($a$) and distribution of the velocity transverse component $W$ ($b$).).

diagram of the computational domain and main components of the vortex system.

The simulations were performed within the model of averaged Reynolds-Favre equations with the Spalart-Allmaras turbulence model. For this purpose, we used proprietary software package ARES [10] which was developed and implemented at KIAM RAS. Paper [8] describes the mathematical model and numerical algorithm in more details. The simulations were performed on the multiprocessor hybrid supercomputer system K-60 in the Supercomputer Centre of Collective Usage of KIAM RAS [11].

Formation of secondary vortices is associated with the boundary layer separation on the main wing under the impact of the generator's tip vortex. Analysis of the gas-dynamic parameters distribution immediately ahead of the wing leading edge allows us to determine possible separation regions. Fig. 2 presents the distribution of pressure $P$ and transverse component of velocity $W$ in the cross-section ahead of the leading edge. Here the pressure in the tip vortex region is approximately 2 times lower than in the surrounding flow. Above the edge there is a region of negative values of transverse velocity, which means that here the flow is directed towards the plane of symmetry ($z = 0$). Particles leaving the vortex region (low-pressure region) are then subjected to an unfavorable pressure gradient. This may promote separation in the vicinity of point $A$ shown in Fig. 2, *b*. This region is somewhat shifted with respect to the vortex center towards the plane of symmetry. For similar reasons, separation may be expected beneath the wing in the vicinity of point $B$

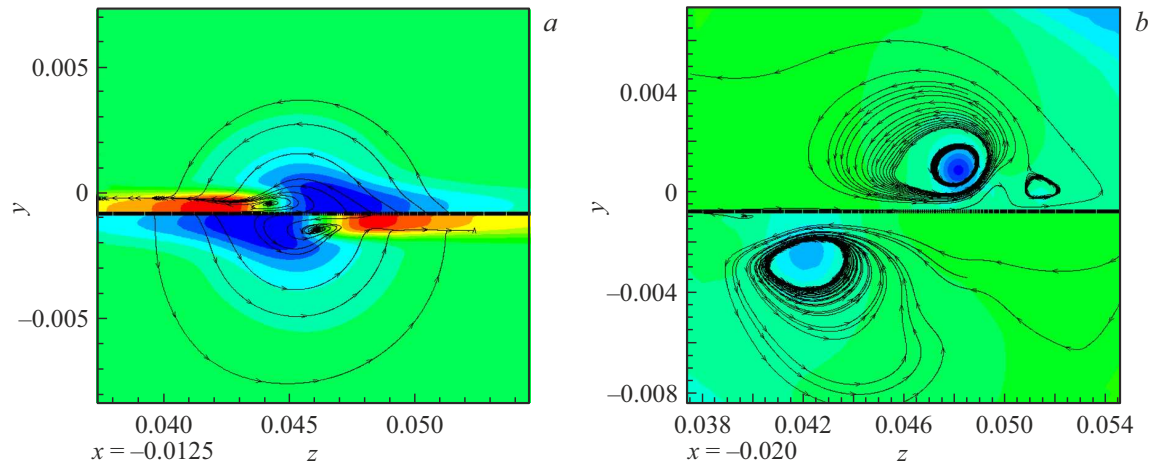


**Figure 3.** Pressure distribution and particle trajectories in cross-sections $x = -0.0125$ ($a$) and 0.02 m ($b$), the case of symmetrical intersection with the wing.

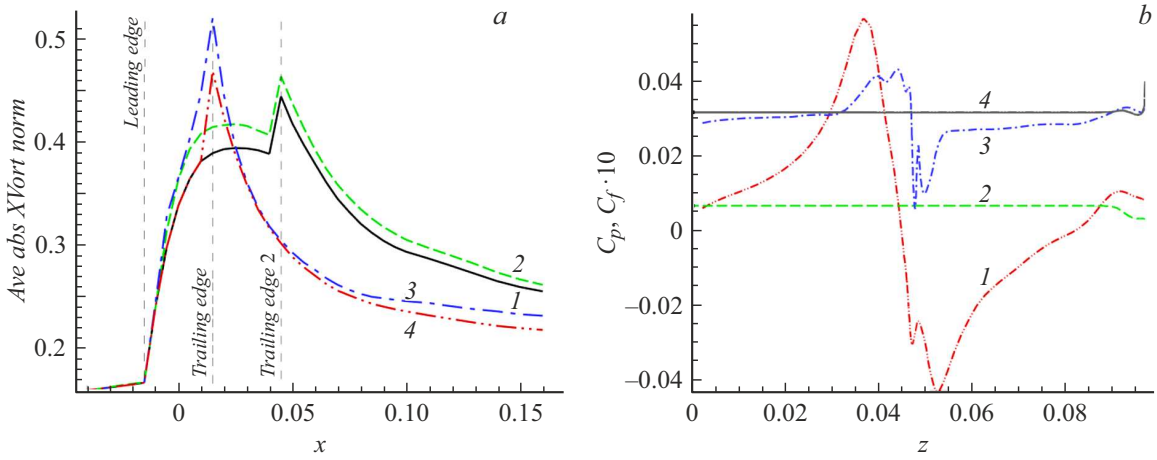


**Figure 4.** $a$ — normalized mean $|\Omega_x|$ versus longitudinal coordinate $x$: Option 1 (*1*), Option 2 (*2*), for the profiled wing (*3*) and for flat wing (*4*). $b$ — distributions of pressure coefficient $C_p$ and friction coefficient $C_f \cdot 10$ along the span in cross-section $x = 0$ m: $C_p$ for Option 1 (*1*), $C_p$ for the uniform free stream (*2*), $C_f \cdot 10$ for Option 1 (*3*), $C_f \cdot 10$ for the uniform free stream (*4*).

shown in Fig. 2, *b*. This region is shifted towards the main-wing tip edge. The presented qualitative considerations are confirmed by the results of numerical modeling. Indeed, in cross-section $x = -0.0125$ m (2.5 mm downstream from the leading edge, Fig. 3, *a*) the center of the circulation flow region is located at point $z \sim 0.0442$ m above the main wing and at point $z \sim 0.0461$ m below the main wing. In this case, the tip vortex axis ahead of the leading edge has coordinate $z \sim 0.452$ m. In subsequent downstream cross-sections, the upper vortex region shifts towards the tip edge, while the lower one shifts towards the plane of symmetry (Fig. 3, *b*). In fact, in cross-section $x = 0.02$ m (Fig. 3, *b*) the center of the circulation flow region is located at point $z \sim 0.0481$ m above the main wing and at point $z \sim 0.0423$ m below it. This fact is consistent with the general theory of vortex-plane interaction [12] and with the options of flows described in [13].

In cross-sections $x = \text{const}$ passing through the rectangular wing, the main contribution to total vorticity $|\Omega| = (\Omega_x^2 + \Omega_y^2 + \Omega_z^2)^{1/2}$ is made by component $\Omega_z$ associated with the boundary layer generation. To quantify the transformation of tip vortex and emerging secondary vortices, the $|\Omega_x|$ value averaged over the cross-section is used. Fig. 4, *a* presents this quantity normalized to the absolute value of the free stream velocity. Starting from the leading edge ($x = -0.015$ m), this value increases sharply due to large values of the modulus of transverse velocity derivative $|\partial w/\partial y|$. Further, as secondary vortices are being generated, this value continues increasing with some decrease in the angular coefficient after passing the wing center. Immediately downstream the tip edge ($x = 0.045$ m) a jump is observed, which is associated, similarly to the case of leading edge, with an increase in $|\partial w/\partial y|$.

Subsequently, while moving downstream, a smooth attenuation of vortex structures occurs under the influence of dissipative factors. However, $|\Omega_x|$ remains significantly higher than in the tip vortex ahead of the leading edge

Flat wing aerodynamic coefficients

| Option | $m_z$ | $C_y$ |
|---|---|---|
| 1 | $5.510 \cdot 10^{-5}$ | $-2.191 \cdot 10^{-4}$ |
| 2 | $9.897 \cdot 10^{-5}$ | $-9.689 \cdot 10^{-5}$ |
| Constant flow | 0 | 0 |

up to the output bound of the computational domain. For Option 1 (symmetrical intersection), $|\Omega_x|$ is slightly higher than in the asymmetrical case. In turn, $|\Omega_x|$ for the profiled wing is slightly higher than for the flat one.

The tip vortex affects all the parameters of the flow around the rectangular wing. For instance, the distributions of pressure coefficients $C_p$ and friction coefficients $C_f$ differ from those in the undisturbed-flow mode as shown in Fig. 4, *b* presenting the distributions of these coefficients over the wing span in cross-section $x = 0\,\text{m}$ (0.25 of the chord downstream the leading edge). For ease of perception, coefficient $C_f$ is scaled tenfold. Extrema in curves $C_p(z)$ and $C_f(z)$ reflect the arrangement of separation regions.

Redistribution of pressure and friction over the surface subjected to the tip vortex leads to violation of the flow symmetry with respect to the wing plane and, hence, to variations in the aerodynamic coefficients (see the Table). Moment $M_z$ was calculated relative to the leading edge.

Thus, the paper analyzes the tip vortex deformation and mechanism for the secondary vortex formation during its interaction with the lifting surface in supersonic flow. We have revealed that interaction between the tip vortex and lifting surface during the boundary layer separation gives rise to two secondary vortices, i. e., the vortex itself gets subdivided into two parts shifting as follows: the upper one towards the trailing edge, the lower one towards the plane of symmetry. Formation of secondary vortices leads to an increase in vorticity $|\Omega_x|$ for all the considered options.

### Funding

The study was supported by the Russian Science Foundation (project 24-21-00230).

### Conflict of interests

The authors declare that they have no conflict of interests.

## References

[1] C. Breitsamter, Prog. Aerosp. Sci., **47** (2), 89 (2011). DOI: 10.1016/j.paerosci.2010.09.002
[2] A.S. Ginevsky, A.I. Zhelannikov, *Vikhrevye sledy samoletov* (Fizmatlit, M., 2008). (in Russian)
[3] V.V. Vyshinsky, G.G. Soudakov, Tr. MFTI **1** (3), 73 (2009); (in Russian) A.V. Bobylev, G.G. Soudakov, V.A. Yaroshevsky, V.V. Vyshinsky, J. Aircraft, **47** (2), 663 (2010). DOI: 10.2514/1.46432
[4] J.M. Luckring, Aeronaut. J., **123** (1264), 729 (2019). DOI: 10.1017/aer.2019.43
[5] C. Chen, Z. Wang, I. Gursul, Exp. Fluids, **59**, 82 (2018). DOI: 10.1007/s00348-018-2539-7
[6] C.J. Barnes, M.R. Visbal, P.G. Huang, J. Fluid Mech., **799**, 128 (2016). DOI: 10.1017/jfm.2016.320
[7] C.J. Barnes, M.R. Visbal, R.E. Gordnier, Phys. Fluids, **27**, 015103 (2015). DOI: 10.1063/1.4905479
[8] V.E. Borisov, T.V. Konstantinovskaya, A.E. Lutsky, Math. Mod. Comput. Simul., **15** (1), 59 (2023). DOI: 10.1134/S2070048223010040.
[9] T. Tadin, M.A. Brutyan, Y. Htun, Tech. Phys. Lett., **50** (12), 24 (2024). DOI: 10.61011/TPL.2024.12.60343.6459k.
[10] V.E. Borisov, A.A. Davydov, I.YU. Kudryashov, A.E. Lutsky, *Programmnyi komplex ARES dlya rascheta trekhmernykh turbulentnykh techeniy vyazkogo szhimaemogo gaza na vysokoproizvoditel'nykh vychislitel'nykh sistemakh*, svidetel'stvo o registratsii programmy dlya EVM RU 2019667338 (23.12.2019). (in Russian)
[11] TsKP IMP RAN [Electronic source]. (in Russian) http://ckp-rf.ru/ckp/670139/
[12] P.G. Saffman, *Vortex dynamics* (Cambridge University Press, 1992).
[13] T.L. Doligalski, C.R. Smith, J.D.A. Walker, Annu. Rev. Fluid Mech., **26**, 573 (1994). DOI: 10.1146/annurev.fl.26.010194.003041

*Translated by EgoTranslating*